Journal of Asian Earth Sciences 168 (2018) 48–56

Contents lists available at ScienceDirect

Journal of Asian Earth Sciences

journal homepage: www.elsevier.com/locate/jseaes

Quantifying gas hydrate from microbial methane in the South China Sea

Jiliang Wang[a,*], Shiguo Wu[a,b], Yongjian Yao[c]

[a] Institute of Deep-sea Science and Engineering, Chinese Academy of Sciences, Sanya 572000, China
[b] Laboratory for Marine Mineral Resources, Qingdao National Laboratory for Marine Science and Technology, Qingdao 266071, China
[c] Guangzhou Marine Geological Survey, Guangzhou 510075, China

ARTICLE INFO

Keywords:
Gas hydrate
South China Sea
Microbial methane

ABSTRACT

Methane hydrate has been confirmed to be present in the South China Sea (SCS) based on drilling expeditions and geophysical indications. It is necessary to access the methane hydrate inventory because of its role in the energy resources and climate change. The aim of this study is to constrain the inventory of methane hydrates in the SCS formed by the microbial degradation of organic matter within the gas hydrate stability zone (GHSZ). Bathymetry, seafloor temperature, and geothermal gradient datasets enabled us to estimate the GHSZ at a resolution of 30″ × 30″ for the SCS. We conclude that the GHSZ occurs at water depths of > 500 m in most areas of the SCS. The methane hydrate distribution formed by microbial methane production in the SCS was computed using the parameterized transfer function recently proposed by Wallmann et al. (2012). The result indicates widespread accumulations of methane hydrate along the continental slopes in the SCS. The microbial methane hydrate is distributed over a 7.69×10^{11} m^2 area and the total abundance of methane hydrate in the SCS is estimated to be 42.8 Gt C.

1. Introduction

Gas hydrates are ice-like solid compounds in which gas molecules are trapped in the cages formed by water molecules at high pressures and low temperatures (Sloan, 1998). Methane is the most common gas found in naturally occurring gas hydrates, and large quantities of methane hydrates are hosted in the shallow sediments of permafrost regions and outer continental margins. In the past decades, gas hydrate has attracted the attenuation of both the scientific community and industrial community due to its role as a future energy supply (Collett, 2002), a factor in global climate change (Dickens et al., 1995) and a submarine geohazard (Nixon and Grozic, 2007).

Gas hydrates are stable only within a limited range of depths called the gas hydrate stability zone (GHSZ). The thickness of the GHSZ is mainly governed by the seafloor temperature, geothermal gradient, water depth, gas composition and pore water salinity in marine settings. Given an adequate gas supply and appropriate reservoir conditions, gas hydrates can accumulate in different morphologies (e.g., pore-filling, fracture-filling) within the GHSZ. The “gas hydrate petroleum system” approach was proposed to guide the gas hydrate exploration and resource evaluation (Collett et al., 2009), in which the GHSZ is a key element because it defines the potential zone of gas hydrate accumulation. In addition, GHSZ analyses is crucial in the assessment of the role of gas hydrates in climate change (Ruppel and Kessler, 2016) and seafloor stability as variations in the GHSZ could cause the dissociation of the methane hydrate.

Both the temperature-pressure conditions and geological conditions are favorable for methane hydrate accumulation in the South China Sea (SCS). Four scientific drilling expeditions, including well logging and sample coring, have been conducted by the Guangzhou Marine Geologic Survey (GMGS), and they have discovered various types of gas hydrates on the northern margin of the SCS (Yang et al., 2017, 2015; Zhang et al., 2014, 2007). A number of studies have presented geological, geophysical and geochemical evidence of the presence of methane hydrate in Southwestern Taiwan, on the continental slope offshore Vietnam and Palawan Trough (Chi et al., 1998, 2006; Chow et al., 2000; Hadley et al., 2008; Lin et al., 2014; Trung, 2012). An oil company also drilled in the Gumusut-Kakap area offshore Borneo to evaluate the geohazard risks and their well logs confirmed the presence of gas hydrates in the deep water area (Hadley et al., 2008). Thus, methane hydrate is present throughout the SCS and it is essential that we estimate the GHSZ in order to aid exploration and assess the quantity of gas hydrates in the SCS.

Many studies have estimated the thickness of the GHSZ and the amount of methane hydrate in the SCS using different approaches. Initially, a variety of methods were used to calculate the thickness of the GHSZ and the amount of gas hydrates in different local areas of the SCS (Chen et al., 2004; Chi et al., 2006; Yao, 2001). After bathymetry

* Corresponding author.
E-mail address: wangjl@idsse.ac.cn (J. Wang).

https://doi.org/10.1016/j.jseaes.2018.01.020
Received 25 April 2017; Received in revised form 17 January 2018; Accepted 17 January 2018
Available online 06 February 2018

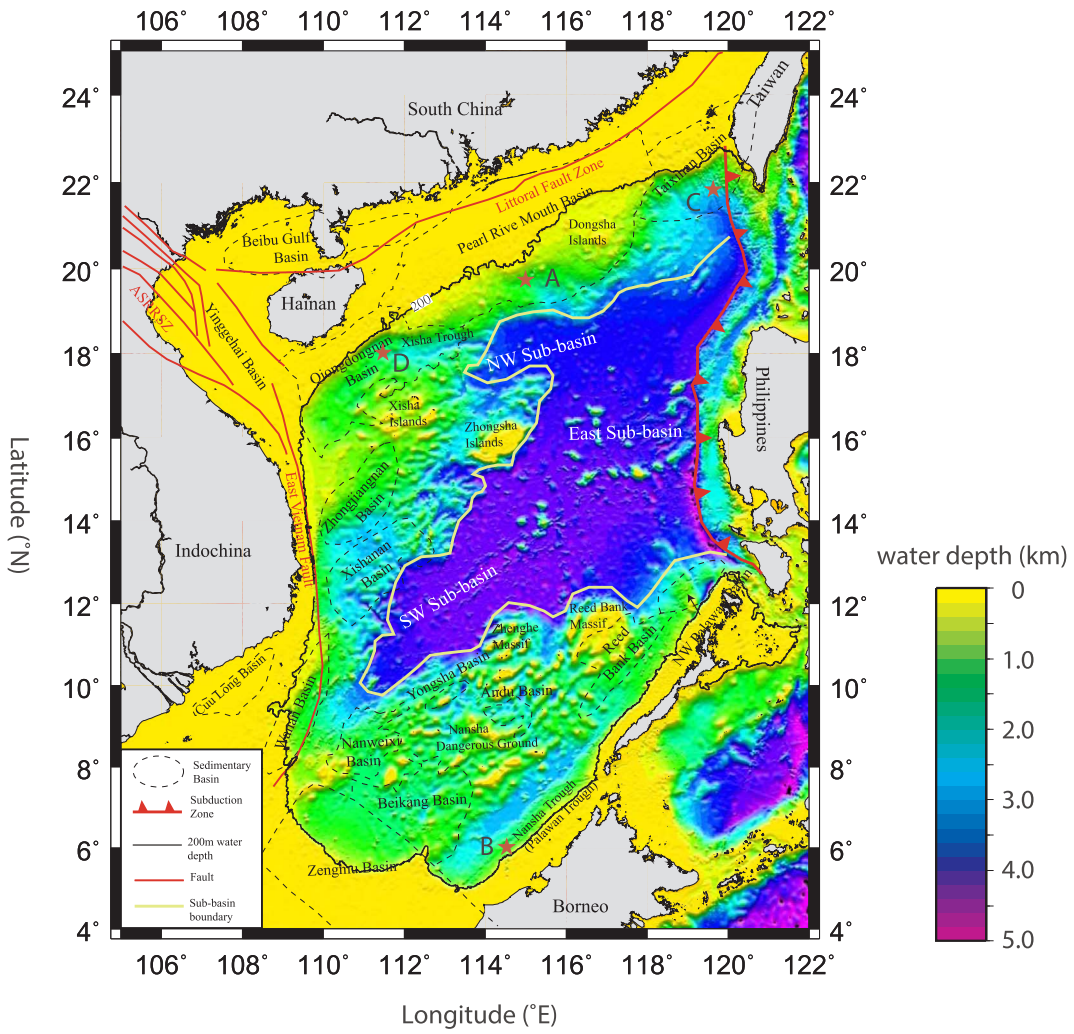

Fig. 1. Bathymetry map of the South China Sea (http://topex.ucsd.edu/WWW_html/srtm30_plus.html) with the main tectonic feathers (Modified from Sun et al. (2009)) overlaid. ASRRSZ: Ailao Shan-Red River Shear Zone. The 200 m water depth contour is overlaid and it generally represents the shelf-slope boundary. Sites A, B, C and D are marked as stars, which are used to evaluate the accuracy of the estimation of the GHSZ (Table 1).

data became available, more attempts were made to estimate the GHSZ of the entire SCS. Wang et al. (2006) calculated the thickness of the GHSZ for three types of gas hydrates using the model proposed by Milkov and Sassen (2001) for the entire SCS. The same method was used with new bathymetry data by Trung (2012) to map the GHSZ in the SCS. These studies used the SCS bathymetry data with a precisions of 1′ × 1′. However, the other two key parameters used lacked precision in both studies. An empirical equation was used to quantify the relationship between water depth and seafloor temperature. A linear function relating the water depth to the geothermal gradient, based on well data for the area, was used to obtain the geothermal gradient of the entire SCS. Thus, in these previous studies, the calculation of the GHSZ mostly depended on the bathymetric data, neglecting regional anomalies and variations in the seafloor temperature and geothermal gradient. More attempts need to be made to improve the precision of previous GHSZ estimations and methane hydrate inventory estimations.

Wallmann et al. (2012) proposed a new approach for constraining the amount of gas hydrate formed from microbial methane production in marine sediments based on a geochemical transport-reaction model. Burwicz et al. (2011) concluded that the amount of methane hydrate formation is mainly controlled by methane supply either through the direct degradation of organic matter within the GHSZ or through an upward flux of deeper biogenic and thermogenic methane. Such gas fluxes have been reported to occur at both active and passive margins, but unfortunately, estimates of methane fluxes from deep sediments are still difficult to constrain. Therefore, only microbial methane hydrate is incorporated in the new model. The model considers the process of methane hydrate formation which is basically controlled by the following key parameters: (1) the accumulation of particulate organic carbon at the seafloor; (2) the kinetics of the microbial degradation of organic matter and methane generation in marine sediments; (3) the thickness of the GHSZ; (4) the solubility of methane in pore fluids within the GHSZ; (5) sediment compaction; (6) the ascent of deep-seated pore fluids and methane gas into the GHSZ. Compared to the previous model (Milkov and Sassen, 2001), the new model takes into account more parameters associated with the process of methane hydrate formation rather than just using the GHSZ and assumed hydrate saturation, resulting in a more realistic result.

This paper is organized as follows: first, new bathymetry data, seafloor temperature data from a high-resolution temperature model of the global ocean and geothermal gradient data interpolated from the Global Heat Database are used to improve the estimation of the GHSZ with a resolution of 30″ × 30″ for the entire SCS; then, we use the method of Wallmann et al. (2012) to evaluate the distribution of methane hydrate throughout the SCS. This estimation should be conducive to further study of the the methane hydrate in the region and provide additional information for other studies.

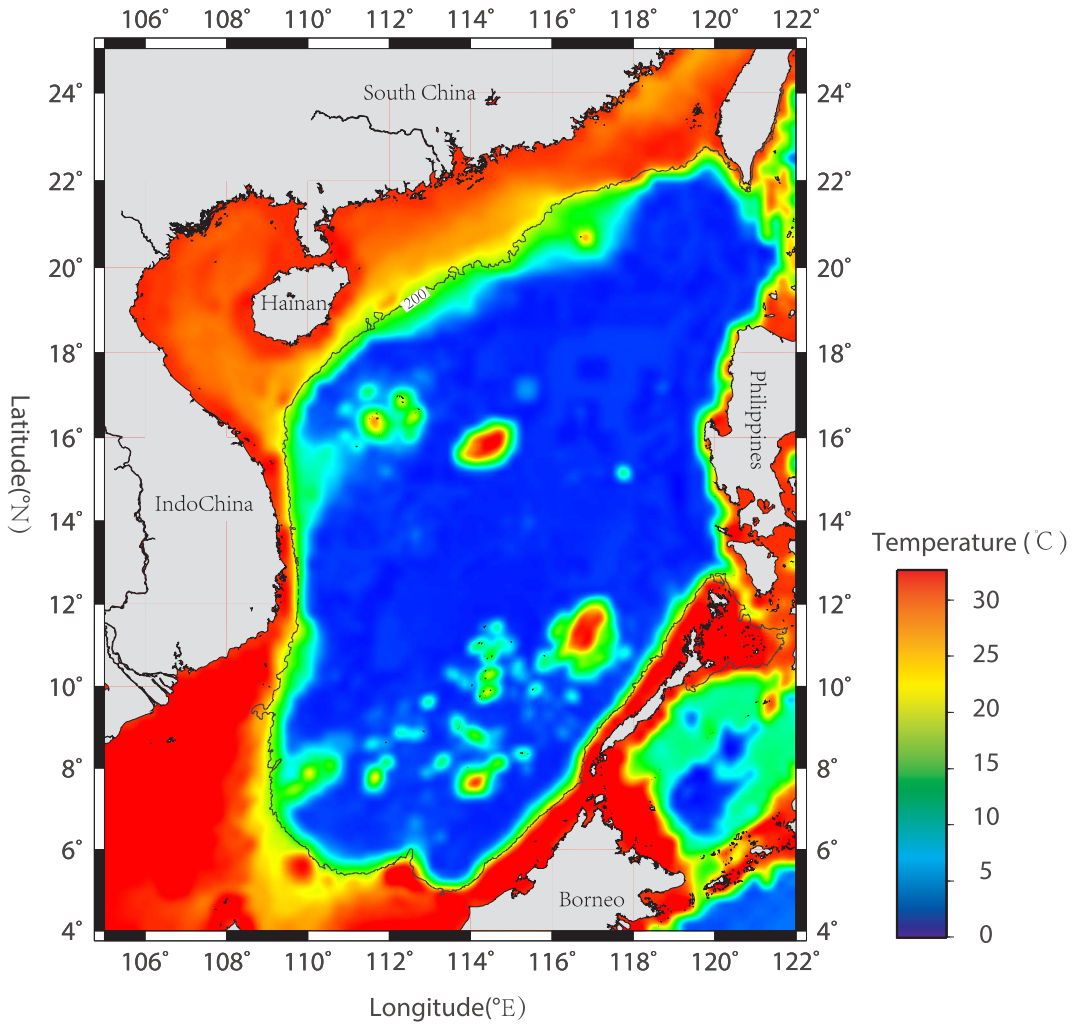

Fig. 2. Seafloor temperature map interpolated from WOA 13 model (https://www.nodc.noaa.gov/OC5/woa13/) on a 30″ × 30″resolution in the South China Sea. The 200 m water depth contour (black line) is overlaid.

2. Geologic setting

The SCS is the largest marginal sea along the Western Pacific with an area of 3.5 × 10^6 km^2 and an average depth of 1350 m. It is located in the juncture between the Eurasian, Pacific, and Indian Plates. The SCS is bounded by different types of continental margins (Briais et al., 1993; Taylor and Hayes, 1983; Zhou et al., 1995) (Fig. 1). The northern edge of the SCS is a rifted continental margin that is separated from the South China block by the littoral fault zone. The western margin of the SCS is bounded by shear faulting indicating a strike-slip extensional margin. On the southern margin, a series of overthrust imbrications have developed from south to north, which is typical of a compressive or convergent continental margin. The eastern margin is connected to the Taiwan-Luzon arc by the Manila trench. The Taiwan-Luzon arc is an active modern island arc formed by the eastward subduction of the SCS basin.

The SCS contains more than 10 Cenozoic hydrocarbon bearing sedimentary basins with a maximum sediment thickness of 14,000 m on the continental shelf and slope (Trung, 2012; Sun et al., 2012, 2017) (Fig. 1). Plenty of organic matter has been carried and injected into the SCS by the rivers of the surrounding continents and islands. Many oil and gas fields are located in this area, such as at the Beibu Gulf Basin, the Pearl River Mouth Basin, and the Wanan Basin. The favorable temperature-pressure conditions, large organic matter supply and thick sediments provide favorable zones for gas hydrate formation, accumulation and storage on the continental slopes of the SCS.

3. Data

Several datasets are required to accurately estimate the distribution of methane hydrate deposits. We compiled the necessary data from various sources. All of the data compiled had a resolution of 30″ × 30″ resolution and covered an area bounded by 105°E ~ 122°E and 4°N ~ 25°N.

Bathymetry, seafloor temperature, and geothermal gradient data are collected to calculate the present-day GHSZ in the SCS under steady state conditions,. The bathymetry data was extracted from the SRTM 30 plus model (http://topex.ucsd.edu/WWW_html/srtm30_plus.html) (Becker et al., 2009). The seafloor temperature used was from the World Ocean Atlas 2013 (WOA13 model; https://www.nodc.noaa.gov/OC5/woa13/). The WOA 13 model includes oceanographic profile data for a 0.25° grid at the standard depth level . In this study, the seafloor temperature data was interpolated on a 30″ × 30″grid from the WOA 13 model (Fig. 2). The geothermal gradient data was compiled from the Global Heat Flow Database of the Internal Heat Flow Commission (http://www.heatflow.und.edu/index2.html) and from Shi et al. (2003) (Fig. 3). Because we directly used the geothermal gradient data, we did not need to assume the thermal conductivity value, which is normally a source of uncertainty (Marín-Moreno et al., 2016). As shown in Fig. 4, 517 sites were used in the compilation. The number of measured sites within the SCS Basin is quite small and the existing sites are mostly anomalous ones because most of them are located in the regional seamount area. In order to obtain a more accurate result, the SCS Basin is

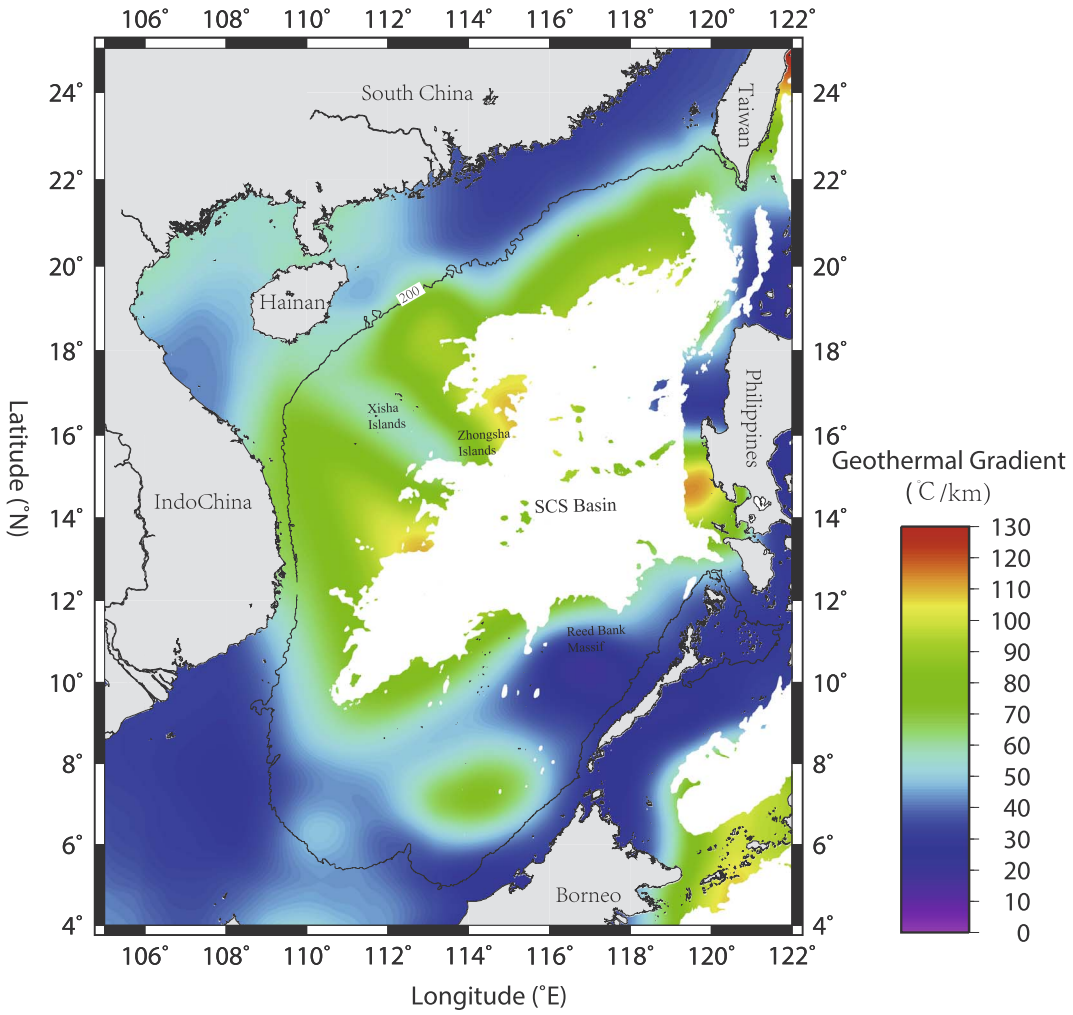

Fig. 3. Geothermal gradient map interpolated from the measured sites shown in Fig. 4 on a 30″ × 30″resolution in the South China Sea. The 200 m water depth contour is overlaid.

excluded when we estimate the GHSZ thickness and the distribution of methane hydrate in the SCS. Another reason to exclude the sea basin is because the sedimentation and the particular organic carbon (POC) accumulation rates are too low, resulting in zero methane hydrate accumulation within the sea basin (Kretschmer et al., 2015). This is consistent with the studies of Wang et al. (2006) and Trung (2012).

4. Methods

4.1. Estimation of the thickness of the GHSZ

The water depth, seafloor temperature, geothermal gradient, water salinity and gas composition are some of the factors that affect the thickness of the GHSZ in marine settings. Here, we assume that the sea water's salinity is 33.5 ppm. With the bathymetry, seafloor temperature and geothermal data as inputs, the GHSZ thickness was computed using Miles (1995) method. The pressure-temperature (P-T) phase diagram for gas hydrate that is for temperature of 0 °C to –30 °C temperature and a sea water salinity of 33.5 ppm can be expressed by a fourth-order polynomial as follows:

$$P = 2.8074023 + 0.1559474 \times T + 0.048275 \times T^2 - 0.00278083 \times T^3 + 0.00015922 \times T^4 \quad (1)$$

,where P is the pressure in MPa and T is the temperature in °C at depth Z below sea level.

The temperature of the sediments at any depth below the seafloor can be defined by the seafloor temperature and the geothermal gradient (dT/dZ) using the following equation:

$$T_Z = T_0 + \frac{dT}{dZ} \times (Z - Z_0) \quad (2)$$

,where $T_0$and $Z_0$are seafloor temperature and seafloor depth, respectively.

The pressure (P) at depth$Z$ is dependent on the water depth, density and gravity acceleration. The hydrostatic pressure-temperature relationship within the sediments is given by:

$$P = [(1 + c_1)Z + c_2 Z^2] \times 10^{-2} \quad (3)$$

,where $c_1 = [5.92 + 5.25 \times \sin^2(Lat)] \times 10^{-3}$and $c_2 = 2.21 \times 10^{-6}$; $Lat$is the latitude in degrees.

Eqs. (1)–(3) were analytically solved using the Newton-Raphson method to obtain the thickness of the GHSZ.

4.2. Quantification of the gas hydrates formed from microbial methane production

The amount of gas hydrate formed from microbial methane production in the SCS was calculated using the transfer functions proposed by Wallmann et al. (2012). The transfer function fits equations to the numerical results using a reactive transport code that considers the dominant physical and biogeochemical processes. The input parameters of the transfer function are the GHSZ, $L_{GHSZ}(m)$, the particulate organic carbon (POC) concentration at the seafloor (wt%), and sedimentation rate (cm/kyr). The methane hydrate inventory, GHI, in kg C/m^2 was

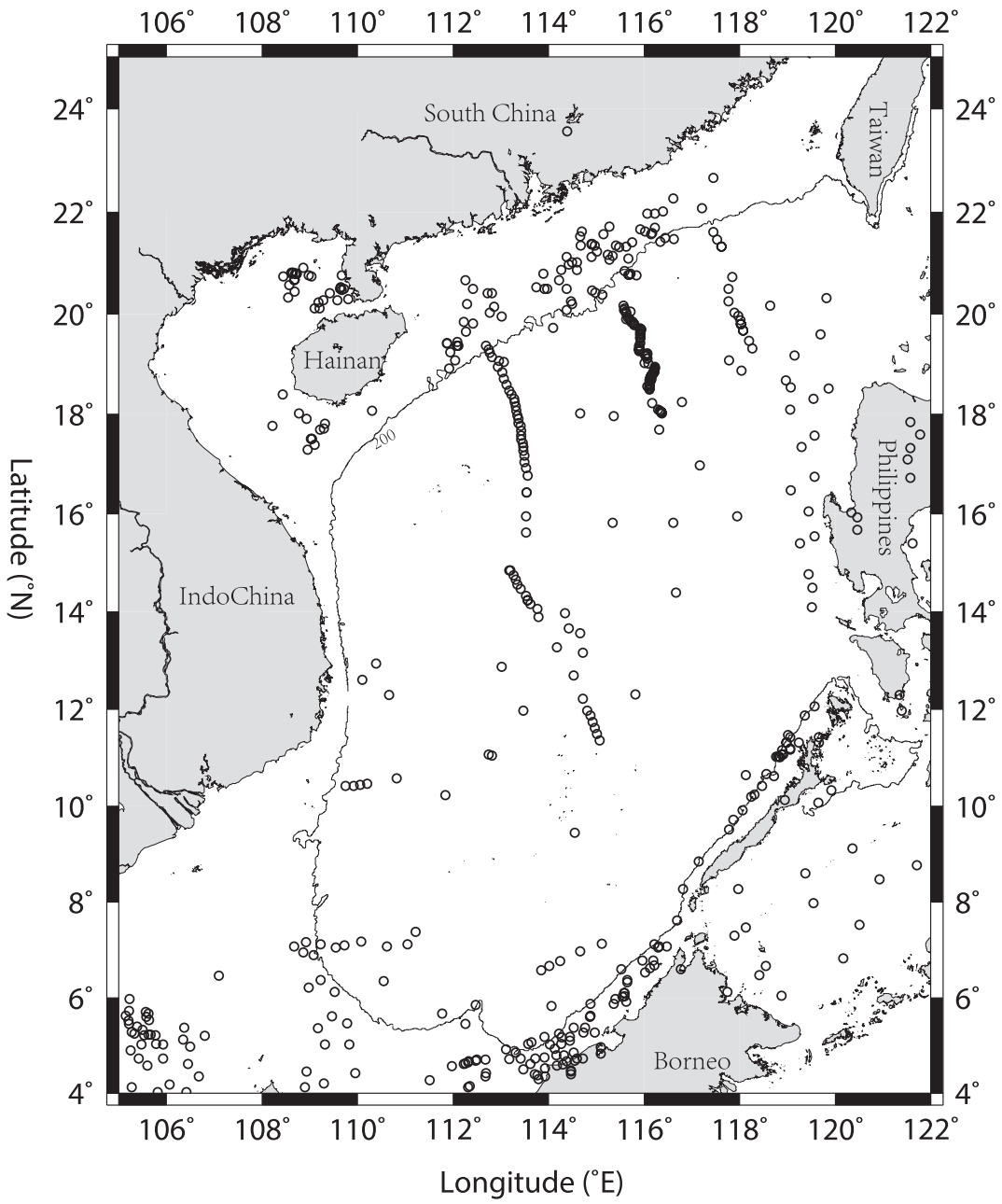

Fig. 4. The measured sites used for compiling the geothermal gradient map in the South China Sea. The data is from the Global Heat Flow Database of the Internal Heat Flow Commission (http://www.heatflow.und.edu/index2.html) and the publication (Shi et al., 2003).

computed at every grid point using the following equation,

$$GHI = a \cdot L_{GHSZ}^{b} \cdot (POC - \frac{c}{w^{d}}) \cdot \exp(-(e + f \cdot \ln(w))^{2}) \quad (4)$$

,

where $a = 0.002848$, $b = 1.681$, $c = 24.42$, $d = 0.9944$, $e = -1.441$ and $f = 0.3925$. The POC concentration at the seafloor is assumed to be 1% (Wallmann et al., 2012). Burwicz et al. (2011) proposed the following parameterized function to compute the sedimentation rate w (in cm/yr) as a function of the water depth z(in m):

$$w = \frac{w_1}{1 + \left(\frac{z}{z_1}\right)c_1} + \frac{w_2}{1 + \left(\frac{z}{z_2}\right)c_2} \quad (5)$$

,with $w_1 = 0.017$ cm/yr, $w_2 = 0.006$ cm/yr, $z_1 = 200$ m, $z_2 = 4000$ m, $c_1 = 3$, and $c_2 = 10$. This equation is valid for computing the sedimentation rates of Holocene surface sediments. Direct observations verify that the thickness of the Holocene sediments is only a fraction of the actual GHSZ thickness. It is therefore more appropriate to consider the mean sedimentation rates averaged over a period of several million years to predict hydrate accumulation.

During glacial periods, the anomalous Holocene shelf accumulation rates (as predicted by Eq. (5)) may have been diminished by an order of magnitude (Hay, 1994). It is therefore reasonable to shift the main deposition area from the shelf to the deeper continental slope and rise. Burwicz et al. (2011) concluded that the sedimentation rate increased over a ~500 km of the continental margins by the transport of deposited material from shelf regions (z = 0–200 m) to the continental slopes. At distance greater than 500 km, Eq. (5) is used to predict the sedimentation rates. Thus, the total amount of sediment supplied to the global ocean stays constant. This modified sedimentation model was used to estimate the inventory of methane hydrate because today's marine hydrate accumulation rates are likely controlled by the

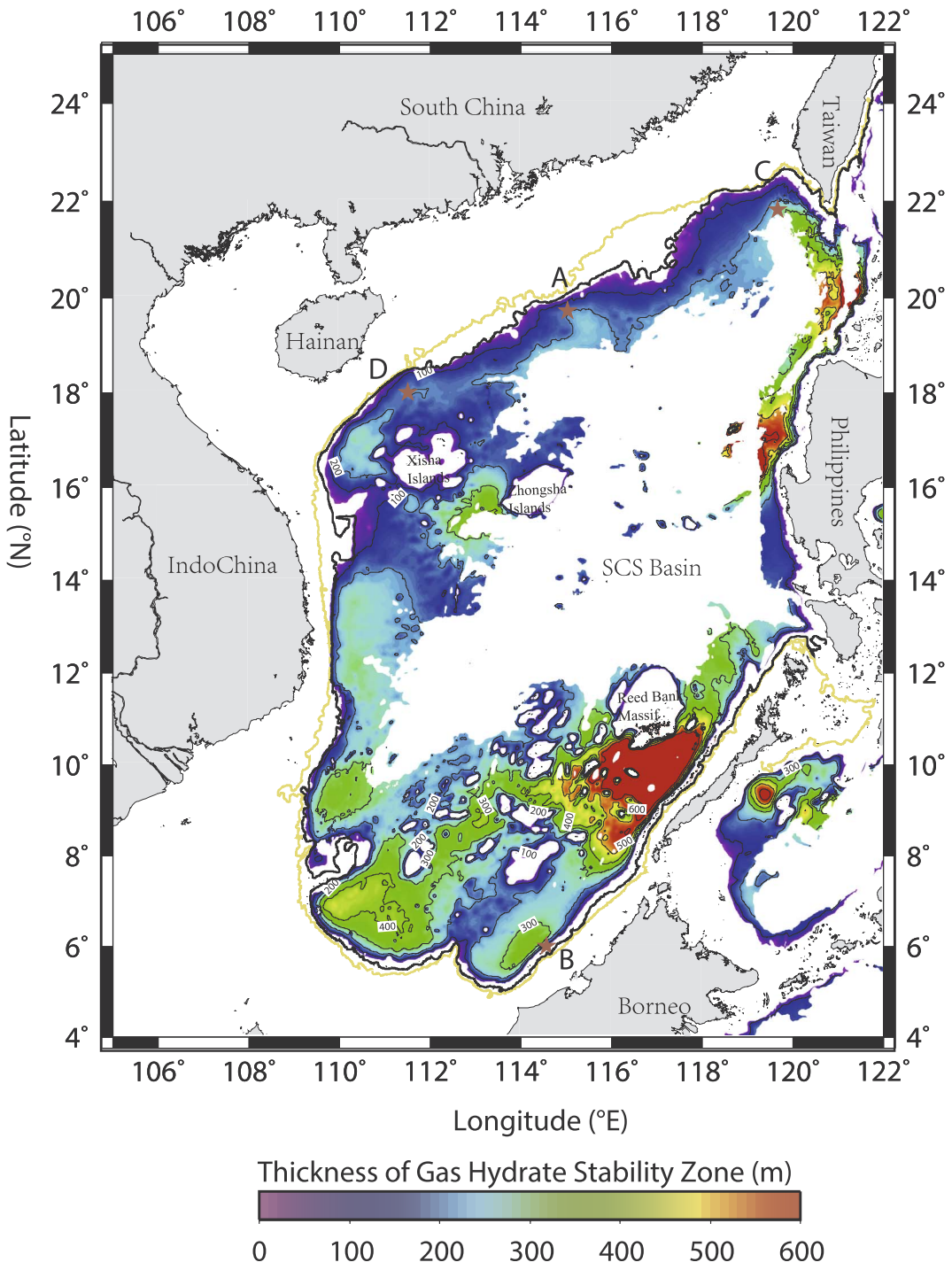

Fig. 5. The thickness of the GHSZ in the South China Sea. Sites A, B, C and D are selected to evaluate the accuracy of the estimation of the GHSZ (Table 1). The 200 m and 500 m water depth are overlaid shown in yellow and black solid lines, respectively.

Quaternary mean values (Wallmann et al., 2012).

5. Result and discussion

5.1. GHSZ thickness map of the SCS

The thickness of the GHSZ is the difference between the base and the top of the GHSZ. Usually the water depth minus the the base of GHSZ is taken to represent the thickness in practical applications. This substitution is reasonable because the methane hydrate is stable at the seafloor as long as the GHSZ exits in the subsurface of the sediment. In several marine settings, methane hydrate nodules have been discovered at the seafloor (Feng et al., 2014; Pape et al., 2011; Sassen et al., 1998; Solomon et al., 2008). It should be noted the relation of the sulfate methane transition zone (SMTZ) and the GHSZ. Methane formed at depth is transported upwards into the SMTZ via molecular diffusion and advection. Within this zone, the methane is oxidized by consortia of bacteria and archaea using sulfate as the terminal electron acceptor (Boetius et al., 2000), which is also known as the anaerobic oxidation of methane (AOM). The AOM can result in the decrease of methane hydrate formation, or even a lack of methane hydrate within the SMTZ. However, the SMTZ is not the top of GHSZ. When the methane supply is

Table 1
Comparisons between the calculated GHSZ and drilling sites/the measured depth of BSR in the SCS.

Location	Drilling wells	Calculated Depth (m)	Depth from Drilling (m)	BSR (m)	Water depth (m)
Shenhu (A)		196.55			~1500
	Sh2		220 (Wang et al., 2011)		
	Sh7		180 (Wang et al., 2011)		
	Sh3		210 (Wang et al., 2011)		
Gumusuk-Kakap (B)		219.07		150–180 (Hadley et al., 2008)	~1200
	Gumusut 2		242 (Hadley et al., 2008)		
	Gumusut 3		175 (Hadley et al., 2008)		
	Gumusut1B		237 (Hadley et al., 2008)		
Southwest Taiwan (C)		267.00		272 (Lin et al., 2014)	~2500
Qiongdongnan Basin (D)		246.30		250 (Wang et al., 2010)	~2000

large enough, methane hydrate can form and exist within SMTZ after the sulfate is used up, which commonly occurs in the active areas of the focused fluid flow.

The map in Fig. 5 shows the calculated thickness of the GHSZ in the SCS. To evaluate the accuracy of our computations, four sites were selected to compare the calculated GHSZ with the drilling results or bottom-simulating reflector (BSR) indicators. Sites A, C and D (Fig. 5) lie on the northern continental margin of the SCS. Site A is located in the Shenhu drilling area. Site B is located in Gumusuk-Kakap, on the southern continental margin of the SCS. Based on the comparisons shown in Table 1, the calculated GHSZ is reliable within a permissible error range.

The main difference between the new map and the previous ones (Trung, 2012; Wang et al., 2006) is that the new GHSZ thickness map is not completely dependent on the water depth. Instead, the geothermal gradient and seafloor temperature also play roles in determining the thickness of the GHSZ. In the Qiongdongnan Basin (Fig. 1), the water depth increases to 1000 m across the break in the shelf-slope; however because of the high geothermal gradient, the thickness of GHSZ is shallower than 250 m. In comparison, the Beikang Basin (Fig. 1) has a GHSZ thickness of greater than 300 m and a 1000 m water depth. Since the seafloor temperature has a strong relationship with water depth (Fig. 2), compared with the geothermal gradient, the effect of the seafloor's temperature on the thickness of GHSZ has the same trend as the water depth.

Some characteristics of the GHSZ map can be speculated from Fig. 5. The GHSZ is widely distributed at the water depth of > 500 m in the SCS. The thickness of the GHSZ is 0–600 m. On most parts of the continental slopes of the SCS, the GHSZ is thinner than 300 m. Generally, the thickness of the GHSZ on the southern continental margin is larger than that on the northern margin because the geothermal gradient of the southern margin is much smaller than that of the northern margin (Fig. 3). For example, the geothermal gradient of the area around Xisha Islands area is greater than 70 °C/km while the geothermal gradient near Reed Bank Massif is less than 50 °C/km. The GHSZ outcrops at a relatively shallower water depth (500 m) on the Western margin of the SCS than in other areas. The shelf is not wide and the slope is steep, resulting in a narrow continental margin in the west. The water depth increases dramatically up to 2 km. Therefore, we tend to believe that the GHSZ outcrop arises at water depths larger than 500 m; however, the slope gradient is so large that the water depth contours (such as 200 m and 500 m) overlap with each other in Fig. 5.

5.2. Methane hydrate distribution in the SCS

Using the predicted GHSZ thickness map, the estimated sedimentation rates, and the assumed POC concentrations of the surface sediments, the distribution of methane hydrate in the marine sediments was calculated using Eq. (4). Methane hydrate has been found by drillings in various morphologies in coarse-grained or fine-grained sediments on the northern and southern continental margins of the SCS. The drilling results also show that the methane trapped in hydrates could have a microbial or thermogenic source. It should be noted that the estimated methane hydrate concentration (Fig. 6) is just a partial estimate of the methane hydrate accumulation in the marine sediments of the SCS because it only takes into account for the hydrate formed from microbial methane production. Fig. 6 shows the methane hydrate concentrations along the continental slopes of the SCS. The shallower (< 500 m) water depths do not contain any methane hydrate because the seafloor temperature is too warm and the pressure is too low. Within the GHSZ, the methane hydrate concentration ranges from 0 to 250 kg C/m^2. On the northern continental margin, the methane hydrate concentration is less than 100 kg C/m^2. On the southern margin, the concentration can reach up to 250 kg C/m^2 in some areas.

The total distribution area and inventory of methane hydrate can be calculated from the estimated hydrate concentration. Based on our results, hydrate formed from microbial methane is distributed over an area of around 7.69×10^{11} m^2. The total inventory of methane hydrate in the SCS is estimated at about 42.8 Gt C. Using an assumed gas hydrate saturation of 1.2%, the methane hydrate volume at STP was estimated to be 1.38×10^{14} by Trung (2012) based on the method of Milkov and Sassen (2001). Our result is approximately half as large as Trung's (2012) estimation. We have discussed the limitations of Trung's (2012) GHSZ estimation in the introduction section. In addition, assuming constant methane hydrate saturation for the entire SCS would introduce additional errors into the estimation. Thus, we conclude that the gas hydrate distribution shown in Fig. 6 and our estimation of the total gas hydrate abundance are more realistic than those of previous results.

6. Conclusions

The SCS has favorable temperature and pressure conditions and large enough organic matter inputs to form and store methane hydrate. The thickness of the GHSZ with a 30″ × 30″ resolution in the SCS was calculated using new compiled data, including bathymetry, seafloor temperature, geothermal gradient. The concentration of the methane hydrate formed from microbial methane was estimated using the parameterized transfer function recently proposed by Wallmann et al. (2012). Methane hydrate is widely distributed along the continental slopes of both the southern and northern continental margins of the SCS. The microbial methane hydrate is distributed over an area of 7.69×10^{11} m^2 and the total abundance of methane hydrate is estimated to be 42.8 Gt C in the SCS. The estimated methane hydrate concentration is just a minimum estimate of the methane hydrate accumulation in the marine sediments of the SCS because it only accounts for the hydrate formed from microbial methane production without considering the gas hydrate from an upward flux of deeper biogenic and thermogenic methane.

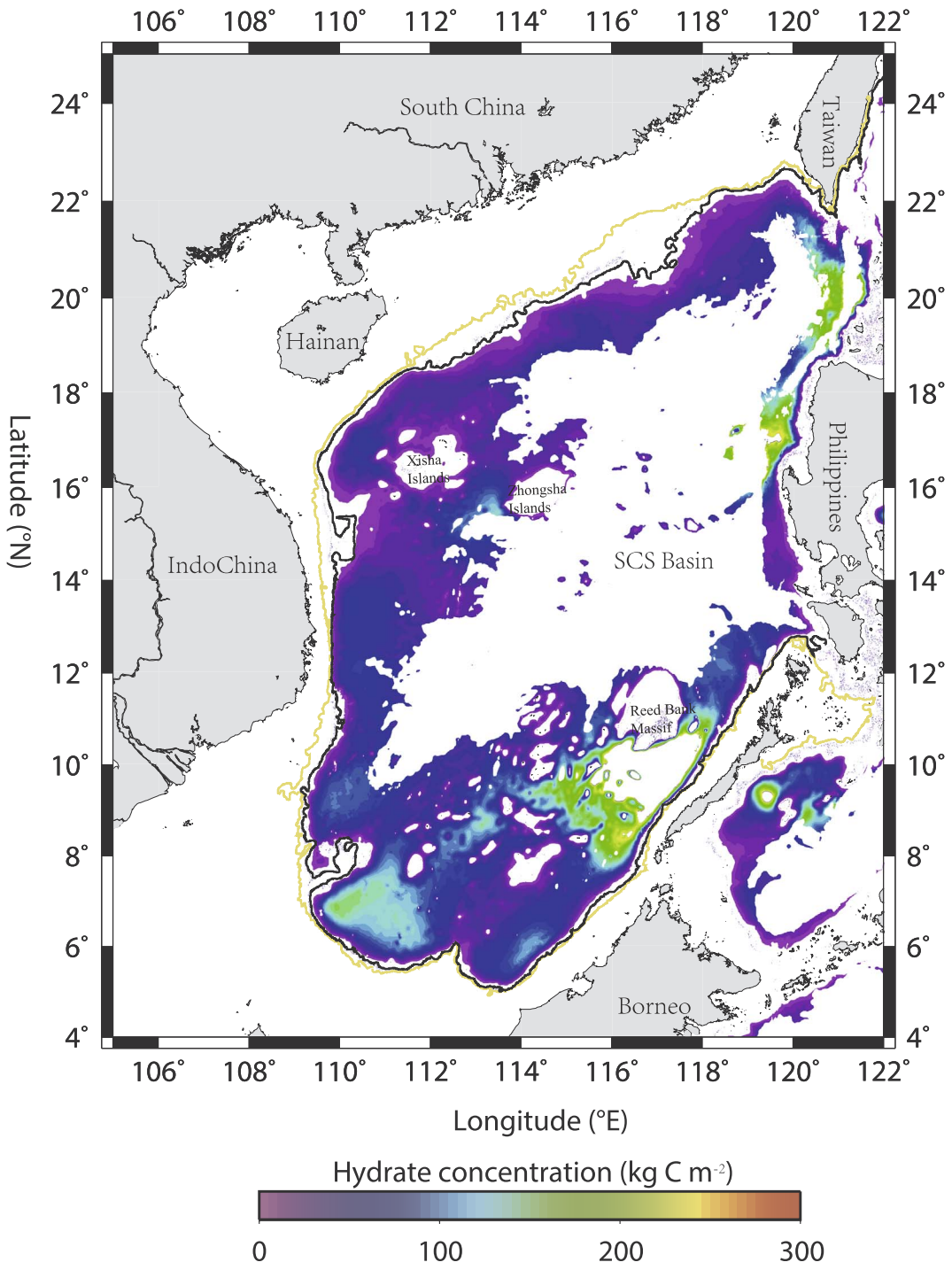

Fig. 6. The methane hydrate concentration (kg C/m^2) formed from microbial methane production in the SCS. For the performed calculations, the sedimentation rates have been obtained according to Eq. (5). The 200 m and 500 m water depth are overlaid shown in yellow and black solid lines, respectively.

Acknowledgements

This work is financially supported by the National Natural Science Foundation of China (No. 41606072), National Program on Key Basic Research Project (973 Program) (No. 2015CB251201), Projects of China Geological Survey (No.s, DD20160227, DD20160227-05), Sanya-Institute Cooperation Project (No. 2016YD34), and State Key Laboratory of Marine Geology, Tongji University (No. MGK 1609). The figures are generated using open-source software Generic Mapping Tools (GMT). We thank Dr. Eva Burwicz, Dr. Dong Feng, and an anonymous reviewer for their detailed and constructive comments.

References

Becker, J., Sandwell, D., Smith, W., Braud, J., Binder, B., Depner, J., Fabre, D., Factor, J., Ingalls, S., Kim, S., 2009. Global bathymetry and elevation data at 30 arc seconds resolution: SRTM30_PLUS. Mar. Geod. 32, 355–371.

Boetius, A., Ravenschlag, K., Schubert, C.J., Rickert, D., Widdel, F., Gieseke, A., Amann, R., Jørgensen, B.B., Witte, U., Pfannkuche, O., 2000. A marine microbial consortium apparently mediating anaerobic oxidation of methane. Nature 407, 623–626.

Briais, A., Patriat, P., Tapponnier, P., 1993. Updated interpretation of magnetic anomalies and seafloor spreading stages in the South China Sea: Implications for the Tertiary tectonics of Southeast Asia. J. Geophys. Res. Solid Earth 98, 6299–6328.

Burwicz, E.B., Rüpke, L., Wallmann, K., 2011. Estimation of the global amount of submarine gas hydrates formed via microbial methane formation based on numerical reaction-transport modeling and a novel parameterization of Holocene

sedimentation. Geochim. Cosmochim. Acta 75, 4562–4576.
Chen, D., Ll, X., Xia, B., 2004. Distribution of gas hydrate stable zones and resource prediction in the Qiongdongnan Basin of the South China Sea.
Chi, W.-C., Reed, D.L., Liu, C.-S., Lundberg, N., 1998. Distribution of the bottom-simulating reflector in the offshore Taiwan collision zone. Terr. Atmos. Ocean. Sci. 9, 779–794.
Chi, W., Reed, D.L., Tsai, C., 2006. Gas hydrate stability zone in offshore southern Taiwan. Terrestrial Atmos. Oceanic Sci. 17, 829.
Chow, J., Lee, J.-S., Sun, R., Liu, C., Lundberg, N., 2000. Characteristics of the bottom simulating reflectors near mud diapirs: offshore southwestern Taiwan. Geo-Mar. Lett. 20, 3–9.
Collett, T., Johnson, A., Knapp, C., Boswell, R., 2009. Natural Gas Hydrates: Energy Resource Potential and Associated Geologic Hazards. AAPG Memoir 89.
Collett, T.S., 2002. Energy resource potential of natural gas hydrates. AAPG Bull. 86, 1971–1992.
Dickens, G.R., O'Neil, J.R., Rea, D.K., Owen, R.M., 1995. Dissociation of oceanic methane hydrate as a cause of the carbon isotope excursion at the end of the Paleocene. Paleoceanography 10, 965–971.
Feng, D., Birgel, D., Peckmann, J., Roberts, H.H., Joye, S.B., Sassen, R., Liu, X.-L., Hinrichs, K.-U., Chen, D., 2014. Time integrated variation of sources of fluids and seepage dynamics archived in authigenic carbonates from gulf of Mexico gas hydrate seafloor observatory. Chem. Geol. 385, 129–139.
Hadley, C., Peters, D., Vaughan, A., Bean, D., 2008. Gumusut-Kakap project: Geohazard characterisation and impact on field development plans. In: International Petroleum Technology Conference. International Petroleum Technology Conference.
Hay, W.W., 1994. Pleistocene-Hocene fluxes are not the Earth's norm. In: Hay, W.W., Usselman, T. (Eds.), Material Fluxes on the Surface of the Earth. National Academy Press, Washington, DC, USA, pp. 15–27.
Kretschmer, K., Biastoch, A., Rüpke, L., Burwicz, E., 2015. Modeling the fate of methane hydrates under global warming. Global Biogeochem. Cycles 29, 610–625.
Lin, C.-C., Lin, A.T.-S., Liu, C.-S., Horng, C.-S., Chen, G.-Y., Wang, Y., 2014. Canyon-infilling and gas hydrate occurrences in the frontal fold of the offshore accretionary wedge off southern Taiwan. Mar. Geophys. Res. 35, 21–35.
Marín-Moreno, H., Giustiniani, M., Tinivella, U., Piñero, E., 2016. The challenges of quantifying the carbon stored in Arctic marine gas hydrate. Mar. Pet. Geol. 71, 76–82.
Miles, P., 1995. Potential distribution of methane hydrate beneath the European continental margins. Geophys. Res. Lett. 22, 3179–3182.
Milkov, A.V., Sassen, R., 2001. Estimate of gas hydrate resource, northwestern Gulf of Mexico continental slope. Mar. Geol. 179, 71–83.
Nixon, M., Grozic, J.L., 2007. Submarine slope failure due to gas hydrate dissociation: a preliminary quantification. Can. Geotech. J. 44, 314–325.
Pape, T., Bahr, A., Klapp, S.A., Abegg, F., Bohrmann, G., 2011. High-intensity gas seepage causes rafting of shallow gas hydrates in the southeastern Black Sea. Earth Planet. Sci. Lett. 307, 35–46.
Ruppel, C.D., Kessler, J.D., 2016. The interaction of climate change and methane hydrates. Rev. Geophys.
Sassen, R., MacDonald, I.R., Guinasso, N.L., Joye, S., Requejo, A.G., Sweet, S.T., Alcalá-Herrera, J., DeFreitas, D.A., Schink, D.R., 1998. Bacterial methane oxidation in sea-floor gas hydrate: significance to life in extreme environments. Geology 26, 851–854.
Shi, X., Qiu, X., Xia, K., Zhou, D., 2003. Characteristics of surface heat flow in the South China Sea. J. Asian Earth Sci. 22, 265–277.
Sloan, E.D., 1998. Gas hydrates: Review of physical/chemical properties. Energy Fuels 12, 191–196.
Solomon, E.A., Kastner, M., Jannasch, H., Robertson, G., Weinstein, Y., 2008. Dynamic fluid flow and chemical fluxes associated with a seafloor gas hydrate deposit on the northern Gulf of Mexico slope. Earth Planet. Sci. Lett. 270, 95–105.
Sun, Q.L., Wu, S.G., Cartwright, J., Shi, H.S., 2012. Shallow gas and its origin in the Pearl River Mouth Basin, northern South China Sea. Mar. Geol. 315–318, 1–14.
Sun, Q.L., Alves, T., Xie, X.N., He, J.X., Li, W., Ni, X.L., 2017. Free gas accumulations in basal shear zones of mass-transport deposits (Pearl River Mouth Basin, South China Sea): An important geohazard on continental slope basins. Mar. Pet. Geol. 81, 17–32.
Taylor, B., Hayes, D.E., 1983. Origin and history of the South China Sea basin. The Tectonic and Geologic Evolution of Southeast Asian Seas and Islands: Part 2 23–56.
Trung, N.N., 2012. The gas hydrate potential in the South China Sea. J. Petrol. Sci. Eng. 88, 41–47.
Wallmann, K., Pinero, E., Burwicz, E., Haeckel, M., Hensen, C., Dale, A., Ruepke, L., 2012. The global inventory of methane hydrate in marine sediments: A theoretical approach. Energies 5, 2449–2498.
Wang, S., Yan, W., Song, H., 2006. Mapping the thickness of the gas hydrate stability zone in the South China Sea. Terrestrial Atmos. Oceanic Sci. 17, 815.
Wang, X., Hutchinson, D.R., Wu, S., Yang, S., Guo, Y., 2011. Elevated gas hydrate saturation within silt and silty clay sediments in the Shenhu area, South China Sea. J. Geophys. Res. Solid Earth 116.
Wang, X., Wu, S., Yuan, S., Wang, D., Ma, Y., Yao, G., Gong, Y., Zhang, G., 2010. Geophysical signatures associated with fluid flow and gas hydrate occurrence in a tectonically quiescent sequence, Qiongdongnan Basin, South China Sea. Geofluids 10, 351–368.
Yang, S., Liang, J., Lei, Y., Gong, Y., Xu, H., Wang, H., Lu, J., Wei, J., 2017. GMGS4 gas hydrate drilling expedition in the South China Sea. Fire in the Ice 17, 5.
Yang, S., Zhang, M., Liang, J., Lu, J., Zhang, Z., 2015. preliminary results of china's third gas hydrate drilling expedition: acritical step from discovery to development in the south China Sea. Center Nat. Gas Oil 412, 386–7614.
Yao, B., 2001. The gas hydrate in the South China Sea. J. Trop. Oceanogr 20, 20–28.
Zhang, G., Yang, S., Zhang, M., Liang, J., Lu, J., Holland, M., Schultheiss, P., 2014. GMGS2 expedition investigates rich and complex gas hydrate environment in the South China Sea. Fire in the Ice 14, 1–5.
Zhang, H.-q., Yang, S., Wu, N., Su, X., Holland, M., Schultheiss, P., Rose, K., Butler, H., Humphrey, G., Team, G., 2007. Successful and surprising results for China's first gas hydrate drilling expedition. Fire in the Ice Newsletter, Fall 9.
Zhou, D., Ru, K., Chen, H.-Z., 1995. Kinematics of Cenozoic extension on the South China Sea continental margin and its implications for the tectonic evolution of the region. Tectonophysics 251, 161–177.